

Enhancement of Gymnastic Movements with Utilizing Strain of Parallel Bars

A.W.S.Chandana^{1*}, Lv Wangang¹, Yi Mingnong¹, and Wei Xubo¹

¹Wuhan Sport University, Wuhan, China

*surajchandana1@gmail.com

Abstract

Gymnasts use a special movement pattern for particular long swing movements to gain optimum elastic energy of parallel bars to complete long swing movements artistically. Therefore it is essential to study body dynamics as well as the dynamic properties of exercise apparatus to minimize the execution errors. In the present study, performance of long swing movement under the parallel bars by national level gymnast of China (mass 50.4 kg) were evaluated. The time history of middle points of wooden bars and all joint angles were measured using a system of ten high speed cameras (100 Hz). The ViconT40 digitizing software was used to find all coordinates of reflective markers (14 mm) which were attached on parallel bar-gymnast system. Based on the overall readings, a 3D mathematical model for the parallel bars apparatus was developed using four damped spring-mass model ($K_x = 28601 \text{ N.m}^{-1}$, $K_Y = 10830$ and $K_Z = 19101 \text{ N.m}^{-1}$) with linear displacement-force characteristics. A gymnast (50.4 kg) applied maximum horizontal force ($F_x=584 \text{ N}$) to perform 'long swing double tucked saltos' to upper arm support on the parallel bars. In this time, the particular vertical force (F_z) and arm angle (α) with X-axis are 488 N and $73^\circ 3'$ respectively. This 3D model can demonstrate dynamic properties of the parallel bars interacting with any long swing movement for any gymnast.

Key words: Dynamic Stiffness, Gymnastic, Long Swing, Model, Parallel Bars

Introduction

The performance on long swing elements on parallel bars is a critical aspect in the Men's Artistic Gymnastics (MAG). This event often increases the difficulty value by players in competitions. Therefore, players pay more attention to the body coordination during the entire long swing movements on wooden parallel bars. When the player reaches the vertical position under the bars, player gains maximum amount of kinetic energy. Hence flexible bars bend and store some of player's energy in response to his actions (in Figure 1). The player gets some of stored elastic energy just before releasing the bars/grips. This energy is most effective to complete long swing elements on the bars artistically. Though most players use common techniques to learn long swing elements, they have to use special body coordination in response to elastic energy of the bars, because parallel bars' movements clearly interact with joint torques of gymnast's body resulting linear and angular momentums. In addition, the tops of the metal posts also interact with long swing movements. Therefore, gymnasts need to consider not only movements of wooden parallel bars but also how tops of metal posts movements interact with the long swing elements to enhance their particular performance.

The elastic properties of parallel bars apparatus play a dominant role in designing artistic gymnastic elements in world class championships and Olympic Games. Players are always searching for the best places of parallel bars to initiate their high difficulty elements on bars. The parallel bars apparatus consists of two bars that are held parallel to, and elevated above, the ground by

a metal supporting framework. Usually these wooden parallel bars are composed of wood with outer coating of wood [FIG, 2009]. Therefore, players use strain of parallel bars and metal posts to generate precise force application for routings on the bars. A player will design his routings based on four different element groups such as swinging skills in a support position, a hanging, an upper arm position and ends with a dismount from either the bars or the side of the wooden parallel bars [FIG, 2017]. Judges mainly evaluate performance of exercises considering of 'difficulty values' and 'execution errors'. If the player is not able to identify the strain of the bars to initiate his high difficult elements on the bars, more execution errors will be occurred through his routings.

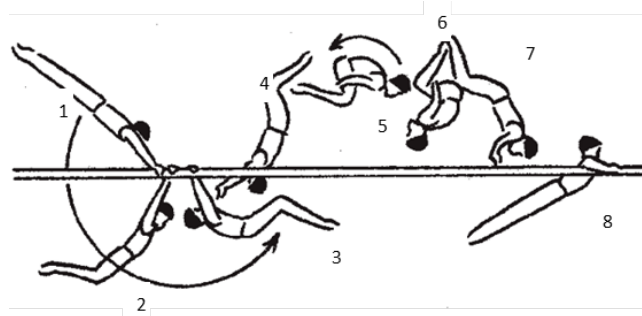


Figure 1: Graphics sequence of an elite gymnast performing with important phases (1 to 8) of 'forward giant swing backward double salto tucked to upper arm hang'

Artistic gymnastic movements which start with long swing under the parallel bars are highly difficult movements compared to other movements of parallel bars

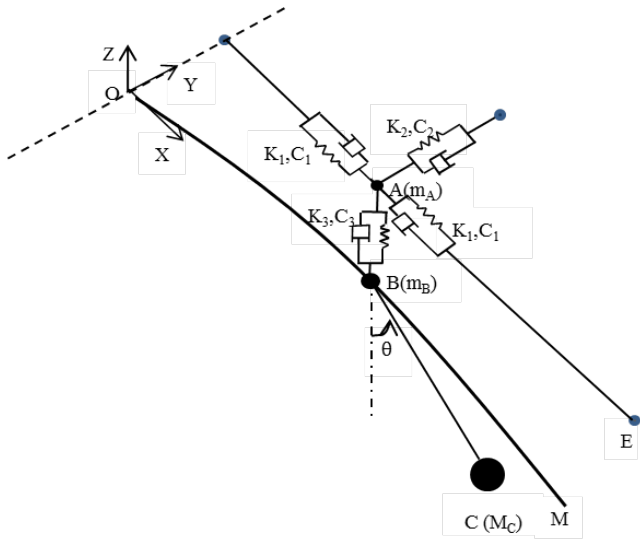


Figure 2: Model for dynamic movement of Parallel bars with three spring-dampers and two point masses m_A and m_B where K_1 , K_2 and K_3 are spring constants and C_1 , C_2 and C_3 are corresponding viscosity coefficients of masses. M_C is attached to mass m_B (at the middle point of a wooden bar) using length l and massless wire. M_C oscillates on YZ plane surface with θ angular displacement at time t . O is an initial position of a top of metal posts and it represents origin of coordinates. F is always moving on sagittal plane with m_A and AF parallel to OY axis. $DE = 230$ cm, $VD = VE$ and D is moveable point on YZ-plane. F can move on the sagittal plane of the parallel bars. LM represents a wooden bar at $t = t$ in the dynamic situation.

apparatus. Because of the variety of evaluations which were introduced by FIG based on long swing movements [FIG, 2017] gymnast has to utilise the strain of the parallel bars in the correct manner. For this aspect, gymnasts use a special movement pattern for particular long swing movements to gain elastic energy of parallel bars to complete long swing movements artistically. The gymnast essentially focused on not only the body dynamic but also the dynamic properties of exercise equipment/apparatus which interact with their movement to minimize the execution errors [Yamasaki *et al.*, 2008]. And also, expert gymnasts state that a slight difference of the apparatus property can affect their performance particularly for advanced techniques, even if the change is within the norm. Some detailed biomechanical model is necessary to assess the various factors influencing performance. As a solution for this problem, biomechanical models can provide important results which are based on performance [Hiley & Yeadon, 2005, Hiley & Yeadon, 2007]. A 2D frontal plane modal for the parallel bars apparatus was developed assuming that the dynamic movements of the tops of the metal posts are negligible [Linge *et al.*, 2006].

Under this study, we have designed a 3D parallel bars

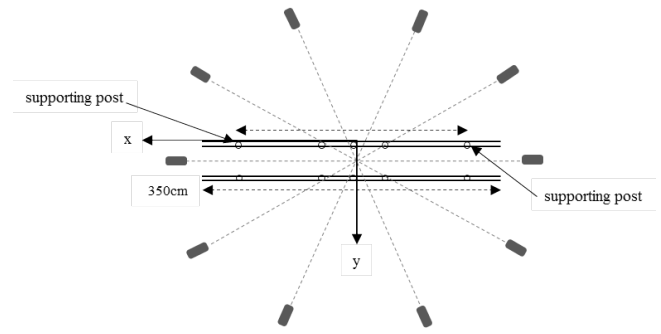


Figure 3: Camera set-up (ViconT40) for data collection viewed from above

model to observe the correct dynamic properties of parallel bars which are engaged in long swing movements and it is compared all observed dynamic properties of parallel bars with apparatus norms introduced by International Gymnastic Federation [FIG, 2009, FIG, 2016]. To create effective force application to perform high difficulty elements under the bars, players and coaches usually observe dynamic strain of wooden parallel bars and four metal pots. In this study, we have calculated dynamic force on bars which is interacting with long swing elements.

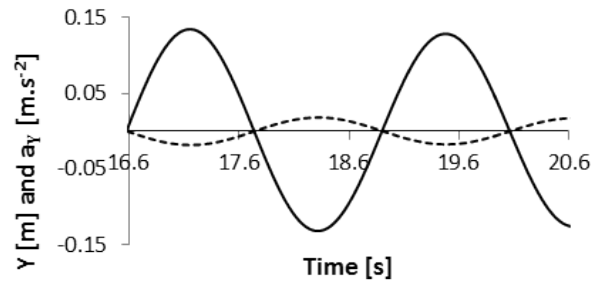


Figure 4: Solid and dashed lines represent acceleration and displacement of m_B in y direction respectively.

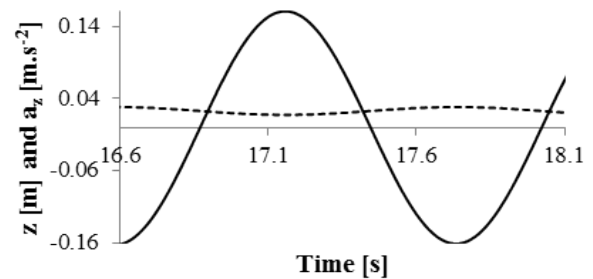


Figure 5: Acceleration (solid line) and displacement of m_B in z direction

Most Olympic players perform highly executed elements on parallel bars without any execution error. That indicates that they know how to get the maximum

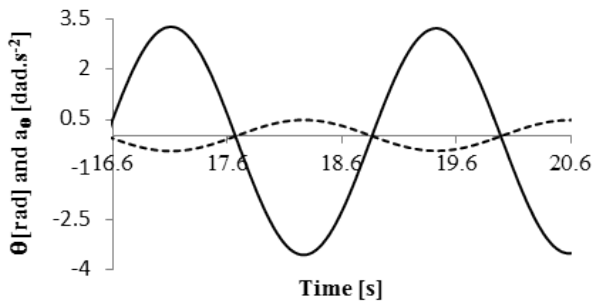


Figure 6: Solid and dashed lines represent angular acceleration and angular displacement of M_c from point B on yz-plane, respectively.

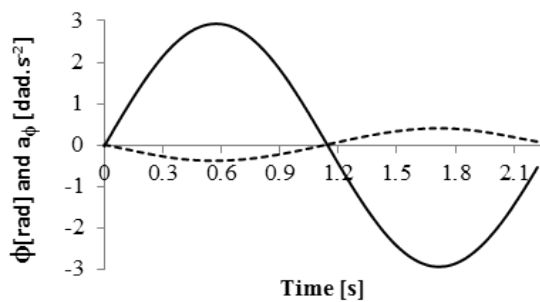


Figure 7: Angular acceleration (solid line) and angular displacement of M_c from point B on xz-plane.

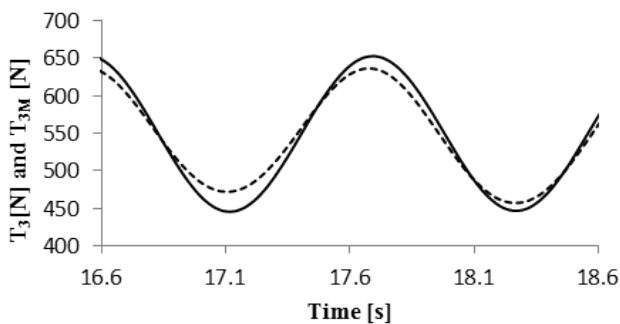


Figure 8: Dynamic force T_3 and its model force T_{3M}

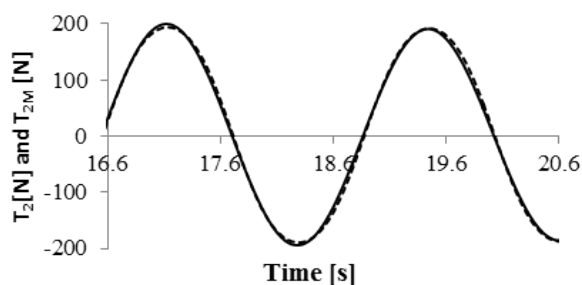


Figure 9: Dynamic force T_2 and its model force T_{2M}

of elastic energy to complete elements on parallel bars. Therefore, the study of 'how elastic energy of bars support gymnasts to perform correctly executed elements on parallel bars in artistic gymnastic?' will help to enhance the players' performance. Though artistic gymnastic elements have been performed by gymnasts taking advantage of elastic energy of parallel bars, they are unable to identify optimum time at which the maximum elastic energy is transferred to a particular movement of gymnastic element. Therefore, most gymnastic players face several difficulties (release phase, momentary phase and injury) to read correct techniques of gymnastic elements. In preparatory period, coaches inform their players to "push" the bars or "pull" the bars, but coaches and players cannot predict the exact value of force and its direction and the time at which it should be done. Hence, gymnast has to get more preparations to perform correctly executed high difficulty elements on parallel bars. To solve this problem, we have designed a 3D mathematical model for parallel bars in a dynamic situation. Hence players and coaches can identify the precise force application relevant to the artistic gymnastic element on parallel bars.

Methods

A 3D mathematical model was designed using four massless spring dampers and two point masses to observe the dynamic properties of wooden bars. This model was hypothesized for parallel bars. Height of the parallel bars from the mat is 175 cm. The Kene's procedure [Levinson & Kane, 1985] was used to derive the system's dynamical equations. In the first part of this study, a pendulum was attached to the middle point of a wooden bar and the oscillations on frontal, sagittal and transverse planes were observed. In the second part of the research, a national level gymnast of China performed four repetitions of a long swing movement on the middle of parallel bars. Hence, kinematic and kinetic values were calculated using Matlab R2014b software and estimated the parameters of spring dampers of mathematical model. Finally, the pattern of dynamic force variation of the middle points of the parallel bars due to the particular long swing movement was calculated.

Mathematical Model of Parallel Bars

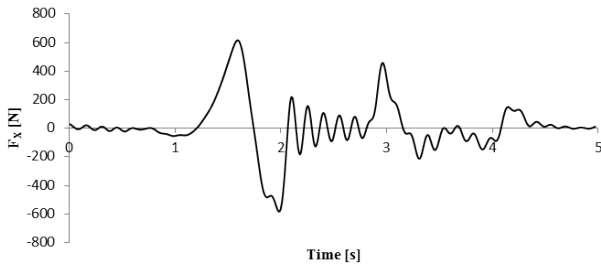
The 3D mathematical model of parallel bars is mainly designed for long swing elements (as in Figure 1). The movements of tops of four metal posts and wooden parallel bars for long swing elements are still not experimentally verified to that how much they influence the performance. The 2D model that indicated the motion of the metal posts in the x-direction (see Figure 2) is very small ($< \pm 1\text{cm}$) compared to much larger gymnast body movements in the sagittal plane [Linge *et al.*, 2006]. We have seen that the tops of metal posts motion in x-direction is not considerably small specially for long swing elements.

Table 1: Results of Parameter Identification of K_y and C_y

Subject(M) [kg]	m_A [kg]	m_B [kg]	K_y [N.m ⁻¹]	C_y [N.s.m ⁻¹]	RMS[N]
50	1.02	5.001	10830	8.975	87.35

Therefore, the middle points of the wooden parallel bars and tops of metal posts movements in three directions were considered to design 3D model for parallel bars' apparatus. The high bar dynamics in the horizontal and vertical directions were represented by linear spring model [Michael & Maurice, 2007]. Four massless spring-dampers and two point masses (A and B in Figure 2) were used to represent parallel bars' dynamic movements from any direction relevant to the long swing elements.

The Kane's method [Levinson & Kane, 1985] was used to derive (Appendix A) following dynamic equations 1 and 2 for above arrangement in Figure 2. T_1 and T_2 are spring-damper forces which are representing the dynamic forces in y and z directions respectively.


Figure 10: Variation of dynamic force (F_x) on middle point A of a wooden bar for artistic gymnastic element in Figure 1

$$T_2 = (m_A + m_B + M_C)\ddot{y} + M_C l [\cos(\theta)\ddot{\theta} - \sin(\theta)\dot{\theta}^2] \quad (1)$$

$$T_3 = (m_B + M_C)(g + \ddot{z}) - M_C l [\sin(\theta)\ddot{\theta} + \cos(\theta)\dot{\theta}^2] \quad (2)$$

Similarly, the dynamic equation 3 was derived considering oscillations of M_C on XZ-plane. The equation 3 represents the horizontal movements of middle point of wooden bars.

$$T_1 = \frac{1}{2} \{ (m + m_B + M)\ddot{x} + ML [\cos(\phi)\ddot{\phi} - \sin(\phi)\dot{\phi}^2] \} \quad (3)$$

Model equations: Vertical (z direction) and horizontal (x and y directions) spring-damper forces are modelled as

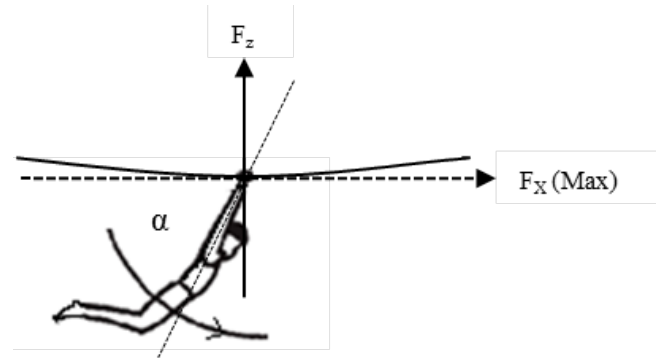
$$T_{1M} = K_x x + C_x \dot{x} + F_x, \quad (4)$$

$$T_{2M} = K_y y + C_y \dot{y} + F_y \quad (5)$$

and

$$T_{3M} = K_z z + C_z \dot{z} + F_z \quad (6)$$

F_x , F_y and F_z are the constant values in each model of the spring dampers. Where K_x , K_y and K_z are the stiffness constants and C_x , C_y and C_z are the constant damping parameters.


Figure 11: A gymnast (50.4 kg) applied maximum horizontal force ($F_x=584$ N) to perform an artistic gymnastic element as in Figure 1 and vertical force (F_z) is 488 N. Arm angle (α) with X-axis is $73^\circ 3'$ on XZ-plane.

Data Collection and Data Processing

Reflective markers (14 mm) and ten high speed camera set up (ViconT40, 100 Hz) were used to observe the time history of the attached markers on parallel bars (in Figure 3) and subjects. The coordinates of the necessary markers were calculated using ViconT40 digitizing software. A 31 kg pendulum was attached to the middle point of a wooden bar using a thin, non-elastic cable. The oscillations on frontal, sagittal and transvers planes were observed. This experiment was repeated for a 50 kg mass pendulum in the same manner. Considering lateral oscillations of pendulum (Appendix), dynamic equations 1 and 2 were formulated. Four reflective markers were attached around the equator of pendulum to observe the time history of its center of mass. In the second part of the research, a national level gymnast of China (50.4 kg) performed four repetitions of a long swing movement: forward giant swing backward double salto tucked to upper arm hang, under four different

Table 2: Results of Parameter Identification of K_z and C_z

Subject(M) [kg]	m_A [kg]	m_B [kg]	K_z [N.m ⁻¹]	C_z [N.s.m ⁻¹]	RMS[N]
50	1.00	5.00	19101	10.9	204.9

Table 3: Results of Parameter Identification of K_x and C_x

Subject(M) [kg]	m_A [kg]	m_B [kg]	K_x [N.m ⁻¹]	C_x [N.s.m ⁻¹]	RMS[N]
50	1.00	5.00	28601	3.9496	0.00019

conditions on the middle of parallel bars. Time histories of all joints of player in dynamic movements were observed using attached markers.

Data Analysis

Parameter Estimations

Parameters m_A , m_B , K_i , and C_i (where $i = \{x, y, z\}$) were estimated using least squares curve fitting (Mathlab14b software) of the formulated spring-damper forces in equations 1, 2 and 3 with their model linear spring-damper forces in equation 4, 5 and 6. Static elastic coefficients of wooden bars were considered for initial values of K_y and K_z to start the estimations¹. The acceleration of gravity is taken to be $g = 9.81 \text{ m.s}^{-2}$. Parallel bar height has been kept as 175 cm from mat.

Model Validation

For validation of parallel bars model, experiment was repeated for each 31 kg and 50 kg pendulums. Hence, estimated values represent similar elastic properties of bars as shown in Table 1, 2 and 3. Also, this experiment was repeated in the same manner for another height of parallel bars (185 cm). In this time, we observed K_x , K_y and K_z as 27633 N.m⁻¹, 10198 N.m⁻¹ and 19512 N.m⁻¹, respectively.

Kinematics of Model

Figure. 4, 5 and 6 show components of accelerations of mA, mB and MC in dynamic equations 1 and 2. Figure 7 shows angular acceleration of mass mA, mB and MC on XZ-plane. Basic calculation steps have been introduced in Appendix .

The Figure 8 and Figure 9 show spring damper forces (dashed lines) and their model values (solid lines). Height of the parallel bars from the mat is 175 cm.

Results and Discussion

The norms of the International Gymnastic Federation demand vertical midpoint stiffness are to be within the range of 19,000-27,400 N.m⁻¹ [FIG, 1996, FIG, 2016, Linge *et al.*, 2006]. In this study, it found the optimum value for vertical midpoint stiffness (K_z) in

the dynamic situation using 50 kg pendulum. We got it in vertical direction as 19,101 N.m⁻¹. The 3D Model of parallel bars estimated other stiffness values for the x direction (parallel to the initial position of a wooden bar) and the y direction as 28,606 N.m⁻¹ and 10,830 N.m⁻¹, respectively. Though the 2D model was designed assuming that the metal posts' movements in the x direction are negligible, we observed that the stiffness values for the x direction (28,606 N.m⁻¹) considerably influenced the long swing movements on parallel bars (see Figure 10). Present study shows special body position in the movement pattern which is near to the second place of sequence in Figure 1 (see Figure 11), is very critical, because the mass 50 kg gymnast can pull the parallel bars in the x-direction to make around 2.2 cm displacement of top of the posts ($-2.3 \text{ cm} < x < +2.3 \text{ cm}$) for three repetitions of the element in Figure 1. In this time, gymnast applied a 584 N force to pull a wooden bar. Hence, gymnast can pull the bars at the bottom of the parallel bars to generate maximum vertical displacement of the middle point of the bars to store maximum amount of elastic energy in wooden bars. Generally, gymnasts know that part of elastic energy will help to lift them above the bars. Therefore, gymnasts do more preparation in long period to gain more energy from the bars. For a solution of this matter, gymnast can design their movement pattern (sequence 1 to 8 in Figure 1) considering the behavior of the new parallel bars model in Figure 2. International Gymnastic Federation (FIG) has introduced and recommended 175 cm standard height of parallel bars from the mat for FIG recommended artistic gymnastic competitions from 2009 to 2016. New Men's Artistic Gymnastics (MAG) code of points in 2017 indicates that the new height of the parallel bars is as 185 cm from the mat. This 10 cm increment of height of parallel bars helps to gain more elastic energy from the bars and metal posts. This directly influences the performance of element. In this study, values of spring constants K_x and K_y of 3D model reduced significantly for 185 cm height of parallel bars from the mat.

Conclusion

The 3D parallel bars model can demonstrate how gymnasts can use dynamic force to complete a 'forward giant swing backward double salto tucked to upper arm hanging on bars with arm support' movement us-

¹International Gymnastic Federation. (2016) FIG Apparatus Norms, Standard Specification for Parallel bars (IV-MAG 5)

ing all three dynamic stiffness values. This 3D model can demonstrate dynamic properties of any long swing movement for any gymnast.

Acknowledgements

We would like to express our thanks to former Gymnastic Olympic Champion (2008) Mr. Yang Wei and Dr Li Shuping for their valuable inputs about the long swing gymnastic movements. Also, our thanks go to a research team in Sports Engineering Department in WSU for assistance during data collection.

References

- International Gymnastic Federation. (1996) FIG Apparatus Norms, Standard Specification for Parallel bars (IV-MAG 5).
- International Gymnastic Federation. (2009) Apparatus Norms (II ed.). Retrieved October 20
- International Gymnastic Federation. (2016) FIG Apparatus Norms, Standard Specification for Parallel bars (IV-MAG 5).
- International Gymnastic Federation. (2017) Code of Point MAG,pp128.
- Hiley, M., and Yeadon, M. (2005) Maximal discounts from high bar. Journal of Biomechanics, v. 38(11),pp2221-2227.
DOI: <https://doi.org/10.1016/j.jbiomech.2004.09.025>
- Hiley, M., and Yeadon, M. (2007) Optimization of Backward Giant Circle Technique on the Asymmetric Bars. Journal of Applied Biomechanics, v. (23),pp300-308.
DOI: <https://doi.org/10.1123/jab.23.4.300>
- Levinson, D. A and Kane, T. R. (1985) Dynamics: Theory and application. New York: McGraw-Hill.
- Linge, S., Hallingstad, O, and Solberg, F. (2006) Modelling the parallel bars in Men's Artistic Gymnastics. Human Movement Science, v. (25),pp221-237
DOI: <https://doi.org/10.1016/j.humov.2005.11.008>
- Michael, J. & Maurice, R. (2007) Optimization of Backward Giant Circle Technique on the Asymmetric Bars. Journal of Applied Biomechanics, v. (23),pp300-3008
DOI: <https://doi.org/10.1123/jab.23.4.300>
- Yamasaki, T, Yamamoto, Y, and Gotoh, K. (2008). A dynamic simulation of high bar movements with bar strain. ISBS conference. Seoul.

Appendix A

The Kene's procedure [Levinson & Kane, 1985] was used to derive the system's flowing dynamical equations 1 and

$$OA = x a_1 + y a_2 ,$$

$$OB = x a_1 + y a_2 - z a_3 \text{ and}$$

$$OC = x a_1 + [y+l \sin(\theta)] a_2 - [z+l \cos(\theta)] a_3$$

Velocities:

$$v^{m_A} = \dot{x}a_1 + \dot{y}a_2$$

$$v^{m_B} = \dot{x}a_1 + \dot{y}a_2 - \dot{z}a_3$$

$$v^{M_C} = \dot{a}_1 + [\dot{y} + l \cos(\theta)\dot{\theta}]a_2 - [\dot{z} - l \sin(\theta)\dot{\theta}]a_3$$

Partial velocities:

$$v_1^{m_A} = \frac{\partial v^{m_A}}{\partial \dot{x}} = a_1$$

$$v_3^{m_A} = \frac{\partial v^{m_A}}{\partial \dot{z}} = a_3$$

$$v_2^{m_B} = \frac{\partial v^{m_B}}{\partial \dot{y}} = a_2$$

$$v_1^{M_C} = \frac{\partial v^{M_C}}{\partial \dot{x}} = a_1$$

$$v_3^{M_C} = \frac{\partial v^{M_C}}{\partial \dot{z}} = a_3$$

$$v_2^{m_A} = \frac{\partial v^{m_A}}{\partial \dot{y}} = a_2$$

$$v_1^{m_B} = \frac{\partial v^{m_B}}{\partial \dot{x}} = a_1$$

$$v_3^{m_B} = \frac{\partial v^{m_B}}{\partial \dot{z}} = a_3$$

$$v_2^{M_C} = \frac{\partial v^{M_C}}{\partial \dot{y}} = a_2$$

Resultant forces:

$$R_1 = R_{m_A} = -T_2 a_2 - (T_3 + m_A g) a_3$$

$$R_2 = R_{m_B} = F \sin(\theta) a_2 + [T_3 - m_B g - F \cos(\theta)] a_3$$

$$R_3 = R_{M_C} = -F \sin(\theta) a_2 + [-M_C g + F \cos(\theta)] a_3$$

Generalized active forces:

$$F_r = \sum_i^2 (v_r^{p_i} \cdot R_i)$$

$$F_1 = v_1^{m_A} \cdot R_1 + v_1^{m_B} \cdot R_2 + v_1^{M_C} \cdot R_3$$

$$F_1 = 0$$

Similarly,

$$F_2 = v_2^{m_A} \cdot R_1 + v_2^{m_B} \cdot R_2 + v_2^{M_C} \cdot R_3$$

$$F_2 = -T_2$$

$$F_3 = v_3^{m_A} \cdot R_1 + v_3^{m_B} \cdot R_2 + v_3^{M_C} \cdot R_3$$

$$F_3 = -T_3 + m_B g + M g$$

Generalized inertia forces:

$$F_1^* = v_1^{p_1} \cdot R_1^* + v_1^{p_2} \cdot R_2^* + v_1^{p_3} \cdot R_3^*$$

$$R_1^* = m_A (\ddot{x}a_1 + \ddot{y}a_2)$$

$$R_2^* = m_A (\ddot{x}a_2 + \ddot{y}a_2 - \ddot{z}a_3)$$

$$R_3^* = M_C \{ \ddot{x}a_1 + (\ddot{y} + l \cos(\theta)\ddot{\theta} - l \sin(\theta)\dot{\theta}^2) a_2 - (\ddot{z} + l \sin(\theta)\ddot{\theta} - l \cos(\theta)\dot{\theta}^2) a_3 \}$$

$$F_1^* = (m_A + m_B + M_C) \ddot{x}$$

$$F_2^* = v_2^{p_1} \cdot R_1^* + v_2^{p_2} \cdot R_2^* + v_2^{p_3} \cdot R_3^*$$

$$F_2^* = (m_A + m_B) \ddot{y} + M_C [\ddot{y} + l \cos(\theta)\ddot{\theta} - l \sin(\theta)\dot{\theta}^2]$$

$$F_3^* = v_3^{p_1} \cdot R_1^* + v_3^{p_2} \cdot R_2^* + v_3^{p_3} \cdot R_3^*$$

$$F_3^* = 0 + m_B \ddot{z} + M_C [\ddot{z} + l \sin(\theta)\ddot{\theta} - l \cos(\theta)\dot{\theta}^2]$$

Dynamic equations:

$$F_1 + F_1^* = 0$$

$$\ddot{x} = 0$$

$$F_2 + F_2^* = 0$$

$$T_2 = (m_A + m_B + M_C) \ddot{y} + M_C [l \cos(\theta)\ddot{\theta} - \sin(\theta)\dot{\theta}^2]$$

(1)

$$\begin{aligned}
 F_3 + F_3^* &= 0 \\
 T_3 &= (m_B + M_C)(g + \ddot{z}) - M_C l [\sin(\theta)\ddot{\theta} + \cos(\theta)\dot{\theta}^2]
 \end{aligned}
 \tag{2}$$

Appendix B

Following calculations were done by considering pendulum movements in YZ-plane. Smooth curve fitting gives z as a function of time t in dynamic movement with minimum RMS value 0.0071. z can fit as $z = A e^{-bt} \sin(\omega t + \phi) + C$ where $A = 0.00645, b = 0.01, \omega = 5.4496, \phi = -0.823$ and $C = 0.0228$. Therefore, second derivative of z in terms of $t(a_z)$ can derive as

$$\ddot{z} = (b^2\omega^2)(z - C) - 2Ab\omega e^{-bt} \cos(\omega t + \phi).$$

Similarly, y can fit as $y = A e^{-bt} \sin(\omega t + \phi) + C$ where $A=0.025901, b=0.01991, \omega=2.70672, \phi=2.2403, C=0.00021$ and RMS value 0.0371. Therefore, second derivative of y in terms of $t(a_Y)$ can derive as $\ddot{y} = (b^2\omega^2)(y - C) - 2Ab\omega e^{-bt} \cos(\omega t + \phi)$. Smooth curve fitting of $\ddot{x} = 0.00386e^{(-0.1871t)} \sin(2.7296t - 6.28) - 0.04294$ and $\ddot{\phi} = 0.3868 \sin(2.752t - 3.1492) + 0.0105$ were done by optimizing parameters of 50 kg pendulum oscillations in XZ-plane. RMS values of them are 1.77×10^{-3} for \ddot{x} and 1.81×10^{-4} for $\ddot{\phi}$.